Therapeutic modulation of the bile acid pool by Cyp8b1 knockdown protects against nonalcoholic fatty liver disease in mice

Chevre, Raphael; Trigueros-Motos, Laia; Castano, David; Chua, Tricia; Corliano, Maria; Patankar, Jay V.; Sng, Lareina; Sim, Lauren; Juin, Tan Liang; Carissimo, Guillaume

Published in:
The FASEB Journal

DOI:
10.1096/fj.201701084RR

Publication date:
2018

THE FASEB JOURNAL • RESEARCH • www.fasebj.org

Therapeutic modulation of the bile acid pool by *Cyp8b1* knockdown protects against nonalcoholic fatty liver disease in mice

Raphael Chevre,[*,1] Laia Trigueros-Motos,[*,1] David Castaño,[*] Tricia Chua,[*] Maria Corlianò,[*] Jay V. Patankar,[†,2] Lareina Sng,[*] Lauren Sim,[*] Tan Liang Juin,[*] Guillaume Carissimo,[‡] Lisa F. P. Ng,[‡,§,¶] Cheryl Neo Jia Yi,[*] Chelsea Chandani Eliathamby,[*] Albert K. Groen,[‖,#] Michael R. Hayden,[*,†] and Roshni R. Singaraja[*,§,3]

[*]Translational Laboratory in Genetic Medicine and [‡]Singapore Immunology Network, Agency for Science, Technology, and Research (A*STAR), Singapore; [†]Department of Medical Genetics, Centre for Molecular Medicine and Therapeutics, Child and Family Research Institute, University of British Columbia, Vancouver, British Columbia, Canada; [§]Yong Loo Lin School of Medicine, National University of Singapore, Singapore; [¶]Institute of Infection and Global Health, University of Liverpool, Liverpool, United Kingdom; [‖]Department of Laboratory Medicine, University of Groningen, University Medical Center Groningen, Groningen, The Netherlands; and [#]Department of Vascular Medicine, Academic Medical Center, University of Amsterdam, Amsterdam, The Netherlands

ABSTRACT: Bile acids (BAs) are surfactant molecules that regulate the intestinal absorption of lipids. Thus, the modulation of BAs represents a potential therapy for nonalcoholic fatty liver disease (NAFLD), which is characterized by hepatic accumulation of fat and is a major cause of liver disease worldwide. Cyp8b1 is a critical modulator of the hydrophobicity index of the BA pool. As a therapeutic proof of concept, we aimed to determine the impact of *Cyp8b1* inhibition *in vivo* on BA pool composition and as protection against NAFLD. Inhibition of *Cyp8b1* expression in mice led to a remodeling of the BA pool, which altered its signaling properties and decreased intestinal fat absorption. In a model of cholesterol-induced NAFLD, *Cyp8b1* knockdown significantly decreased steatosis and hepatic lipid content, which has been associated with an increase in fecal lipid and BA excretion. Moreover, inhibition of *Cyp8b1* not only decreased hepatic lipid accumulation, but also resulted in the clearance of previously accumulated hepatic cholesterol, which led to a regression in hepatic steatosis. Taken together, our data demonstrate that *Cyp8b1* inhibition is a viable therapeutic target of crucial interest for metabolic diseases, such as NAFLD.—Chevre, R., Trigueros-Motos, L., Castaño, D., Chua, T., Corlianò, M., Patankar, J. V., Sng, L., Sim, L., Juin, T. L., Carissimo, G., Ng, L. F. P., Yi, C. N. J., Eliathamby, C. C., Groen, A. K., Hayden, M. R., Singaraja, R. R. Therapeutic modulation of the bile acid pool by *Cyp8b1* knockdown protects against nonalcoholic fatty liver disease in mice. FASEB J. 32, 3792–3802 (2018). www.fasebj.org

KEY WORDS: NAFLD therapeutics · steatosis · liver targeting · siRNA delivery · intestinal cholesterol absorption

Nonalcoholic fatty liver disease (NAFLD) is characterized by the accumulation of lipids in hepatocytes (hepatic steatosis) (1). Twenty to forty percent of patients with NAFLD are affected by the clinically significant form, nonalcoholic steatohepatitis (NASH), which is characterized by inflammatory changes and fibrosis in the liver (1, 2). The prevalence of NAFLD is dramatically increasing worldwide, and NASH-related cirrhosis is expected to become the leading cause of liver transplantation in many developed countries in the near future (3, 4); however, no effective therapies exist for the treatment of NAFLD or NASH.

Bile acids (BAs) are the primary products of cholesterol catabolism. The hydrophilic/lipophilic balance of the BA pool is tightly controlled by different enzymes that modulate BA synthesis in the liver, as well as by the gut microbiome, and is the major regulator of cholesterol homeostasis and intestinal absorption of fat. Immediate products of BA synthesis pathways in humans are the

ABBREVIATIONS: BA, bile acid; CA, cholic acid; CDCA, chenodeoxycholic acid; FXR, farnesoid X receptor; HCD, high-cholesterol diet; KD, knockdown; LDL-C, LDL cholesterol; MCA, muricholic acid; NAFLD, nonalcoholic fatty liver disease; NASH, nonalcoholic steatohepatitis; ORO, Oil-Red-O; siRNA, small interfering RNA

[1] These authors contributed equally to this work.

[2] Current affiliation: Friedrich-Alexander-University Erlangen-Nürnberg (FAU), Universitätsklinikum Erlangen, Erlangen, Germany.

[3] Correspondence: National University of Singapore/Agency for Science, Technology, and Research, 8A Biomedical Grove, Immunos L5, Singapore 138648. E-mail: rsingaraja@tlgm.a-star.edu.sg

doi: 10.1096/fj.201701084RR

This article includes supplemental data. Please visit *http://www.fasebj.org* to obtain this information.

0892-6638/18/0032-3792 © FASEB

primary BAs, cholic acid (CA) and chenodeoxycholic acid (CDCA), and the balance between their relative amounts determines the overall hydrophobicity of the BA pool (5, 6). The major regulator of the balance between CA and CDCA is sterol 12α-hydroxylase (CYP8B1), which adds a 12α-hydroxyl group to 7α-hydroxy-4-cholesten-3-one, thereby determining the relative amounts of 12α- and non–12α-hydroxylated BAs (7). In contrast to humans, CDCA in mice is largely converted to the more hydrophilic muricholic acid (MCA). Conjugation of primary BAs lowers their pK_a and increases their solubility (8). In the gut, the microbiome also plays a critical role in BA pool remodeling by removing both conjugated moieties and hydroxyls to form more hydrophobic secondary BAs. Overall, these processes give rise to a complex assembly of surfactants with different hydrophobicity indexes and different abilities to absorb fat (8, 9). In addition to acting as surfactants, BAs also function as signaling molecules and are the physiologic ligands for nuclear farnesoid X receptor (FXR) (10–12), and the G protein–coupled BA receptor-1 (also known as TGR5) (13–15). As different BAs activate their receptors with different affinities (16), the complexity of the BA pool and the relative amounts of the different BAs determine the signaling properties of the BA pool.

In the last decades, BA sequestrants have been developed to modify the solubilization properties of the BA pool, and have demonstrated their efficacy in metabolic diseases and in lowering LDL cholesterol (LDL-C) (17). Moreover, BA receptors regulate the signaling pathways that are involved in myriad physiologic processes that are impaired in cardiometabolic disorders, such as lipid metabolism (18), glucose homeostasis (18, 19), energy expenditure (20), and hepatic inflammation (21). In this context, BAs emerged as potential therapeutic targets for the treatment of NAFLD (16, 22), and obeticholic acid (6-ethyl-CDCA), a semisynthetic FXR agonist, is currently being investigated in a phase III trial in patients with NASH; however, use of FXR and TGR5 agonists has been restricted as a result of either a lack of efficacy or adverse effects (23, 24).

CYP8B1 is responsible for the overall hydrophobicity index of the BA pool, regardless of the secondary modifications of BAs that take place within the intestinal tract. In BA feeding experiments in mice, overall hydrophilic/lipophilic balance of the bile salt pool, and not the individual fed BAs, *per se*, is the critical determinant of cholesterol absorption from the small intestine (9). Of note, in this study, feeding of 12α-BAs increased the absorption of cholesterol compared with that of non–12α-BAs (9). More recently, increased plasma levels of 12α-hydroxylated BAs have been associated with human insulin resistance (25), and insulin regulates hepatic lipid metabolism *via* modulation of BA levels (26). Moreover, abolished CA synthesis in different *Cyp8b1*$^{-/-}$ mouse models increased the global BA pool (27), reduced atherosclerosis (28), and improved insulin sensitivity (29). In addition, mouse and human studies demonstrated a critical role for Cyp8b1 and 12α-hydroxylated BAs in the regulation of lipid metabolism and fatty liver development (30–33). Of interest, the ratio of 12α- and non–12α-hydroxylated BAs is increased in patients with NAFLD (33), which suggests that a decrease in CYP8B1 may be associated with protection against NAFLD.

Recent advances have demonstrated the potential of RNAi targeting of the liver as a treatment strategy for metabolic diseases, such as NAFLD (34–36). Synthetic nanovectors are lipid- or polymer-based nanoscale particles that are used to deliver hydrophobic drugs, proteins, and nucleic acids—pDNA, RNA or small interfering RNA (siRNA)—*in vivo* (37). Gene-based methods have suffered from the insufficient control of dosage, risk of genomic integration, and antiviral immune responses. Modified siRNAs or antisense oligonucleotides in which one or more nucleotides are modified to increase their stealth properties represent an alternative therapeutic platform with great potential (35).

In this study, we aimed to establish a therapeutic proof of concept for the treatment of NAFLD by targeting hepatic *Cyp8b1* by using nonviral delivery of modified siRNA *in vivo* to modulate the BA pool and increase its metabolically protective biologic properties. We achieved effective, long-term knockdown (KD) of hepatic *Cyp8b1*, which led to a profound remodeling of the BA pool. We demonstrate that this remodeling dramatically reduces lipid accumulation in the liver and inhibits NAFLD.

MATERIALS AND METHODS

Animals and diets

Female C57BL/6N mice age 2–5 mo were used in this study. Animals had *ad libitum* access to water and were fed with a standard chow diet (Altromin 1324 Mod) or a high-cholesterol diet (HCD; 0.5%; Harlan Diets, Madison, WI, USA) for 10–20 wk, beginning at age 2 mo. Mice were unfed for 5 h before any procedures. Plasma for all experiments was isolated from blood that was drawn from the saphenous vein in EDTA-coated capillary tubes. Feces were collected continuously over 72 h. All experiments were approved by the Institutional Animal Care and Use Committee at the Agency for Science, Technology, and Research.

In vitro siRNA screening

HEK293T cells were maintained at 37°C in 5% CO_2 and DMEM (Sigma-Aldrich, St. Louis, MO, USA) that was supplemented with 10% heat-inactivated fetal bovine serum (GE Healthcare, Chalfont St. Giles, United Kingdom), 4 mM glutamine, and 1% penicillin/streptomycin. Twenty-four hours after seeding, cells were transiently cotransfected with a plasmid that encoded murine *Cyp8b1* and 6 different siRNAs (Origene, Rockville, MD, USA; and Thermo Fisher Scientific, Waltham, MA, USA) by using Lipofectamine 2000 according to the manufacturer's instructions (Thermo Fisher Scientific).

In vivo inhibition of *Cyp8b1*

Cyp8b1 siRNA (sense: CGGCAUAAGCUGUUGGUUAtt, antisense: UAACCAACAGCUUAUGCCGtc) or negative control siRNA (*In Vivo* Ready siRNA; Thermo Fisher Scientific) and Invivofectamine 3.0 (Thermo Fisher Scientific) complexes were prepared according to manufacturer instructions. Either PBS, control or *Cyp8b1* siRNA-Invivofectamine solution (dose, 0.5 or 1

mg siRNA/kg mouse) was administered *via* tail vein injection to wild-type mice for the indicated period of time.

Gene expression analyses

Total RNA was isolated from tissue homogenates by using an RNeasy Kit (Qiagen, Valencia, CA, USA). cDNA was generated by using random hexamers and a Superscript III First-Strand Synthesis Kit (Thermo Fisher Scientific). Quantitative real-time PCR was performed by using SYBR Green PCR Master Mix (Applied Biosystems, Carlsbad, CA, USA) in an ABI QuantStudio 6 Flex Real-Time System. Reactions were performed in technical triplicates by using the following primers: *mCyp8b1* (for *in vivo* studies): (forward) 5′-ATCGCCTGAAGGCCGTGCAG-3′, (reverse) 5′-AGCTGGGGAGAGGAAGGAGTGC-3′; *mCyp8b1* (for cotransfection studies): (forward) 5′-CCTCTGGAGAAGGGTTTTGTG-3′, (reverse) 5′-GCACCGTGAAGACATCCCC-3′; m*Cyp7a1*: (forward) 5′-ACGCACCTCGTGATCCTCTGGG-3′, (reverse) 5′-GGCTGCTTTCATTGCTTCAGGGCT-3′; *mFgf15*: (forward) 5′-AGACGATTGCCATCAAGGACG-3′, (reverse) 5′-GTACTGGTTGTAGCCTAAACAG-3′; *mFgfr4*: (forward) 5′-CTCGATCCGCTTTGGGAATTC-3′, (reverse) 5′-CAGGTCTGCCAAATCCTTGTC-3′; *mFXR*: forward: 5′-TCCAGGGTTTCAGAGACTGG-3′, (reverse) 5′-GCCGAACGAAGAAACATGG-3′; *mSHP*: (forward) 5′-TGGGTCCCAAGGAGTATGC-3′, (reverse) 5′-GCTCCAAGACTTGACACAGTG-3′; *mActin*: (forward) 5′-ATGCTCCCCGGGCTGTAT-3′, (reverse) 5′-CATAGGAGTCCTTCTGACCCATT-3′; *mGapdh*: (forward) 5′-TGTGTCCGTCGTGGATCTGA-3′, (reverse) 5′-TTGCTGTTGAAGTCGCAGGAG-3′; *mRpl37*: (forward) 5′-GGAGTGCCAAGGCTAAGAGAC-3′, reverse: 5′-TCTGAATCTGCGGTAGACAATCT-3′; *mHprt1*: (forward) 5′-AGTGTTGGATACAGGCCAGAC-3′, (reverse) 5′-CGTGATTCAAATCCCTGAAGT-3′; *mTbp*: (forward) 5′-CCTTGTACCCTTCACCAATGAC-3′, (reverse) 5′-ACAGCCAAGATTCACGGTAGA-3′. Relative quantification of gene expression was performed by using the geometric mean of β-actin, glyceraldehyde-3-phosphate dehydrogenase (*Gapdh*), ribosomal protein L37 (*Rpl37*), hypoxanthine phosphoribosyltransferase 1 (*Hprt1*), and TATA binding protein (*Tbp*) as internal controls. Quantitative PCR results were analyzed by using the comparative C_t method (38).

Western blot

Mouse liver samples were homogenized in 300 μl RIPA buffer that was supplemented with complete protease inhibitors (Roche Diagnostics, Mannheim, Germany), and lysates were solubilized in Laemmli sample buffer. Proteins were resolved on a precast polyacrylamide gel (Bio-Rad, Hercules, CA, USA), then transferred to PVDF membranes, blocked with 5% skim milk, and probed with anti-Cyp8b1 (clone P18; Santa Cruz Biotechnology, Dallas, TX, USA) or anti-calnexin (Sigma-Aldrich) Abs overnight. After incubation with horseradish peroxidase–conjugated secondary Abs (Santa Cruz Biotechnology), membranes were developed by using chemiluminescence (Bio-Rad). Relative densities of the proteins of interest *vs.* the housekeeping protein, calnexin, were calculated from the percent area under the curve generated by using ImageJ (National Institutes of Health, Bethesda, MD, USA).

Oral fat tolerance test

Blood was drawn from unfed mice before and after—1, 2, and 4 h—intragastric gavage of 200 μl of corn oil. Plasma triglycerides were measured by using a LabAssay Triglyceride Kit (Wako Pure Chemicals, St. Louis, MO, USA).

Liver histopathology

For conventional light microscopy, livers from *Cyp8b1* siRNA-treated or control mice were fixed in 4% paraformaldehyde for 36 h, dehydrated, and embedded in paraffin. Sections (5 μm thick) were deparaffinized and subjected to routine hematoxylin and eosin staining or Sirius red staining. Lipid droplets in the liver were stained by using the lysochrome Oil-Red-O (ORO) method. In brief, liver slices were washed in 1× PBS and fixed as previously described. Livers were sequentially cryoprotected in 15 and 30% sucrose until tissues sank. Thereafter, liver slices were included in labeled cryomolds using optimum cutting temperature compound (VWR Chemicals, Radnor, PA, USA) and cryosectioned in 12-μm sections (Micron HM525; Thermo Fisher Scientific). ORO stock solution was prepared by magnetic stirring of 2.5 g ORO (Sigma-Aldrich) in 400 ml of isopropanol for 2 h at room temperature. Bright-field images were captured with a light microscope (Axiovision; Zeiss, Oberkochen, Germany) at ×20 magnification, and lipid accumulation was quantified by use of ImageJ. For visualization of cholesterol crystals and macrophages, tissues and slides were prepared according to the cryopreservation protocol previously described. For macrophages, antigen retrieval steaming in Dako Target Retrieval Solution S1699 (Dako, Carpinteria, CA, USA) was performed, and samples were blocked and stained overnight with the anti-F4/80 Ab (MCA497G, 1:400; Bio-Rad). Sections were then washed, incubated for 1 h with fluorescently tagged secondary Ab, and mounted with a water-soluble mounting medium after washing. Cholesterol crystals were detected by using polarized light signals as previously described (39).

Flow cytometry

Fifteen microliters of EDTA blood was washed in PBS before red blood cell lysis for 5 min on ice, followed by washing in PBS. Cells were stained for viability (Supplemental Table 1) for 30 min on ice, washed with PBS, and then blocked for 20 min in blocking buffer (1% rat serum; Sigma-Aldrich). Cells were then stained for 20 min with an Ab mix (Supplemental Table 1). After washing Abs with PBS, data were acquired on a Lsr5 flow cytometer (Becton Dickinson, Franklin Lakes, NJ, USA), and data analysis was performed by using FlowJo (v.10 10.1; FlowJo, Ashland, OR, USA).

Lipid extraction from liver and feces

Mouse liver samples or feces (10 mg) were homogenized in 300 μl PBS, and lipids were extracted with equal volume of chloroform: isopropanol:NP-40 (7:11:0.1). After vortexing, samples were incubated in a rotor wheel for 1 h and spun at 15,000 *g* for 10 min. Organic phase was collected and air dried, and the lipid pellet was resuspended in isopropanol.

BAs, lipids, and hepatic enzymes quantification

BA levels in plasma were analyzed by LC-MS, and total BAs in feces were measured by using the Total Bile Acid Assay Kit (Cell Biolabs, San Diego, CA, USA) according to manufacturer instructions. Plasma alanine transaminase, aspartate transaminase, HDL cholesterol, LDL-C, and total cholesterol were measured by using Cobas c311 system (Roche Diagnostics). Liver and fecal content of cholesterol and triglycerides was measured from lipid extracts as previously described by using an Infinity Cholesterol Kit (Thermo Fisher Scientific) and LabAssay Triglyceride Kit, respectively.

Statistical analysis

Results are expressed as means ± SEM, and statistical significance was evaluated by using Student's *t* test, except when indicated. Curves in **Fig. 3*A*** were compared by using 2-way ANOVA, followed by Sidak's multiple comparison test. Curves in Supplemental Fig. 3 were compared by using a log-rank (Mantel-Cox) test. Statistical significance was calculated by using Prism (GraphPad Software, La Jolla, CA, USA). Values of $P < 0.05$ were considered statistically significantly different.

RESULTS

siRNA administration efficiently inhibits *Cyp8b1* expression *in vivo*

Cyp8b1 is a critical modulator of the hydrophilic/lipophilic balance of the BA pool, which makes it a tightly regulated protein. Indeed, multiple signaling pathways and physiological conditions affect its expression, such as fasting, food intake, and circadian rhythms (40, 41), which allows levels of Cyp8b1 to double during the course of a single day (40). This high turnover of the Cyp8b1 protein is necessary to rapidly adapt the BA pool to changing energy intake and needs. Thus, inhibition of *Cyp8b1 in vivo* for therapeutic purposes by using transient methods may represent a challenge, as sustained inhibition may be required to achieve long-term alterations in the BA pool to impact metabolic phenotypes. To achieve long-term *Cyp8b1* KD and BA pool remodeling, we first screened 6 different siRNAs that targeted *Cyp8b1* (si1–6) *in vitro*, and identified 3 candidates that displayed similar levels of protein KD 48 h after transfection (Supplemental Fig. 1). Of the 3, we selected si1 (**Fig. 1*A*** and Supplemental Fig. 1) and evaluated its transfection efficiency *in vivo* by using Invivofectamine 3.0, which promotes efficient KD in the liver without triggering significant inflammation (42). We administered either control or si1 siRNA (1 mg/kg i.v.) in wild-type mice, and found that hepatic Cyp8b1 protein expression was inhibited at d 2 postinjection (Fig. 1*B*). To assess the kinetics of Cyp8b1 KD, we evaluated levels of Cyp8b1 RNA (Fig. 1*C*) and protein (Fig. 1*D, E*) at different time points and found that injection of 1 mg/kg si1 was sufficient to efficiently knock down Cyp8b1 protein by >75% for 4 d (Fig. 1*D, E*); however, as expected, Cyp8b1 expression rapidly increased to reach its initial mRNA and protein levels within 5 d postinjection (Fig. 1*C–E*). *Cyp8b1*$^{+/-}$ mice present milder BA pool remodeling compared with *Cyp8b1*$^{-/-}$ mice (32), which suggests that a high level of long-lasting KD is required to fully remodel the BA pool. To maintain long-term Cyp8b1 KD, we designed a multi-injection protocol, performing a second injection of 0.5 or 1 mg/kg si1 3 d after the first injection of 1 mg/kg si1 (**Fig. 2*A–C***). We observed dose-dependent KD in *Cyp8b1* expression. The second administration of 0.5 mg/kg si1 allowed for a 50% KD at the protein level, but mRNA levels remained unaffected for up to 6 d after the first injection (Fig. 2*A–C*); however, the second injection of 1 mg/kg si1 achieved a 50% inhibition at the RNA level (Fig. 2*A*) and a >90% inhibition of Cyp8b1 at the protein level for up to 6 d after the first injection (Fig. 2*B, C*). Thus, we successfully designed a twice-per-week injection protocol that allowed for the maintenance of >90% KD of Cyp8b1 protein over longer-term studies.

Cyp8b1 silencing reduces 12α-hydroxylated BA production and promotes BA pool remodeling

As Cyp8b1 critically modulates the 12α-/non–12α-hydroxylated BA ratio, we first determined whether the 6-d KD of Cyp8b1 affected this balance. The injection protocol that used 1 mg/kg at d 0 and 3 led to a 59% reduction in plasma 12α-hydroxylated BAs (control: 0.831 μM; and *Cyp8b1* siRNA: 0.341 μM) and a 69% decrease in the ratio of 12α-/non–12α-hydroxylated BA (Fig. 2*D* and Supplemental Fig. 2). Similar to *Cyp8b1*$^{-/-}$ mice (29), mice that were injected with *Cyp8b1* siRNA demonstrated alterations in the composition of the BA pool (Supplemental Fig. 2), with significantly lower levels of CA and increased levels of MCAs. This indicates that our siRNA multi-injection protocol is sufficient to almost completely remodel the BA pool.

To evaluate the functional consequences of changes in the BA pool composition, we next assessed its signaling properties. Cyp7a1 is the rate-limiting enzyme in the BA synthetic pathway, and its expression is regulated in mice by the Fxr–Shp axis in the liver and by the intestinal secretion of Fgf15 (43, 44). Of interest, BA pool changes that are driven by *Cyp8b1* KD were associated with a significant increase in *Cyp7a1* transcript levels (Fig. 2*E*), recapitulating the phenotype described in *Cyp8b1*$^{-/-}$ mice (27). We found no significant changes in hepatic *Fxr* and *Shp*, and a mild increase in liver *Fgfr4* (Fig. 2*E*), which is the hepatic receptor for Fgf15; however, we observed significant down-regulation in *Shp*, along with a trend toward a decrease in *Fgf15* in the intestine (Fig. 2*E*).

Thus, our longer-term silencing of *Cyp8b1* promoted the remodeling of the BA pool, along with changes in its signaling properties.

Cyp8b1 KD reduces intestinal lipid absorption and circulating LDL-C levels

To evaluate the potential therapeutic applicability of *Cyp8b1* KD on metabolic diseases, such as NAFLD, we next investigated whether the silencing of *Cyp8b1* affects the biologic properties of the BA pool. We performed oral fat tolerance testing after 6 d of silencing, and observed that *Cyp8b1* KD significantly reduced the ability of the BA pool to facilitate the absorption of triglycerides in the digestive system (Fig. 3*A*). As long-term reductions in intestinal fat absorption may be beneficial against hepatic fat accumulation, we determined the impact of *Cyp8b1* KD on fat absorption in a chronic setting by feeding mice an HCD for 15 wk, followed by an additional 3 wk of siRNA injections (2 injections/wk) during which mice continued on HCD. We observed a significant 16% increase in the fecal content of cholesterol in *Cyp8b1* siRNA-treated mice (Fig. 3*B*), which suggested a decrease in intestinal cholesterol absorption. These changes were additionally potentiated by a significant increase in the dry weight of excreted feces

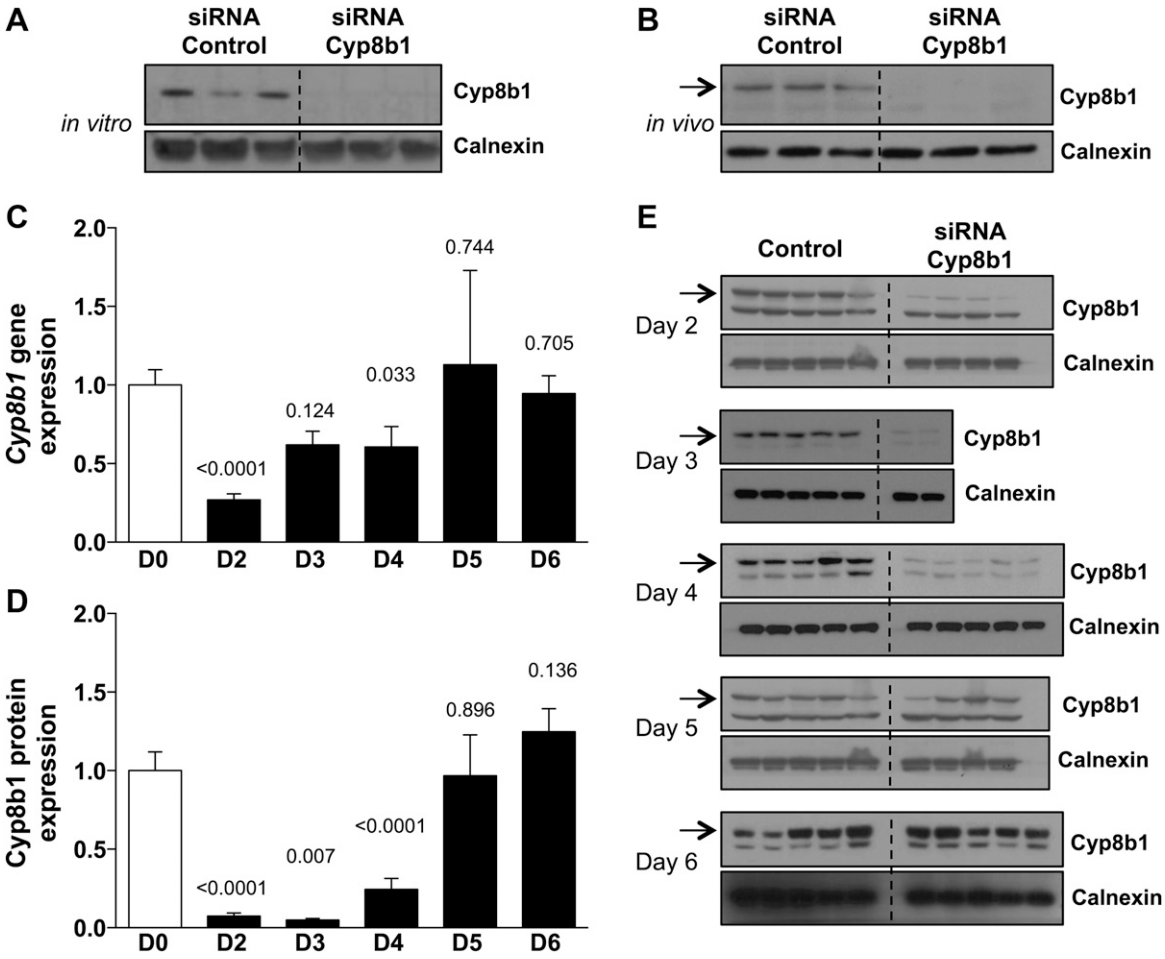

Figure 1. Dynamics of *Cyp8b1* KD. *A*, *B*) KD efficiency of *Cyp8b1* siRNA s1 was evaluated *in vitro* (*A*) and *in vivo* (*B*) in whole liver tissue with respect to siRNA control, and Cyp8b1 protein expression was assessed 2 d after transfection. *C–E*) Wild-type (WT) mice were injected with *Cyp8b1* siRNA si1 or PBS (control group) and *Cyp8b1* RNA (*C*), and protein (*D*, *E*) expression was assessed at d 0–6 postinjection. Expression level of *Cyp8b1* RNA is represented respective to internal controls (*C*). Cyp8b1 protein was normalized to calnexin expression for each group (*D*). Bars represent means ± SEM (n = 2–5 mice). Representative Western blots (*E*). Black arrows (*A*, *B*, *E*) indicate Cyp8b1 protein.

(Fig. 3C), which led to an increase in the overall excretion of cholesterol per day from 10.50 to 13.64 mg (P = 0.001). In addition, an increase in the expression of *Cyp7a1* should result in increased fecal BA content (27). Correlating with increased hepatic expression of *Cyp7a1* that was observed in Fig. 2*E*, fecal BA excretion was increased by 20% (Fig. 3*D*) in *Cyp8b1* siRNA-treated mice. Of interest, these changes were associated with a decrease in plasma LDL-C levels (Fig. 3*E*), without a significant effect on HDL cholesterol levels (data not shown), which mimicked the LDL-C lowering effect of BA sequestrants in humans (17). Taken together, our data indicate that siRNA-mediated *Cyp8b1* KD reduces fat absorption and increases both cholesterol catabolism and cholesterol excretion, which might lead to protection against NAFLD by lowering hepatic lipid accumulation.

Therapeutic silencing of *Cyp8b1* inhibits NAFLD

We next assessed *Cyp8b1* KD as a therapeutic proof of concept for the treatment of NAFLD. We fed mice a diet that was enriched in cholesterol (0.5% w/w; HCD) for 15 wk, followed by 4 additional wk of the HCD diet plus either control or si1 siRNA that targeted *Cyp8b1* (**Fig. 4**). We did not detect any changes in body weights after siRNA treatment (Supplemental Fig. 3). We observed a dramatic 52% reduction in liver steatosis, as assessed by hematoxylin and eosin staining (Fig. 4*A*). During tissue cryopreservation, liver slices from the siRNA-treated group sank in sucrose solution faster than did slices from the control group (median time decreased from 1015 to 137.5 min; $P < 0.0001$; Supplemental Fig. 4), which suggested a decrease in liver fat content. Indeed, livers that were treated with *Cyp8b1* siRNA exhibited significantly lower liver cholesterol content (Fig. 4*B*) and lipid droplet area (Fig. 4*C*), which correlated with a significant decrease in liver triglycerides (Fig. 4*D*). At this time point and in this model, no significant fibrosis was observed in either the siRNA or control groups (Fig. 4*E*), and no changes in collagen could be detected between both groups (Fig. 4*E*). In addition, a significant decrease in the liver/body weight ratio was observed (Fig. 4*F*). We assessed the silencing of Cyp8b1, as well as 12α- and non–12α-BA levels and BA

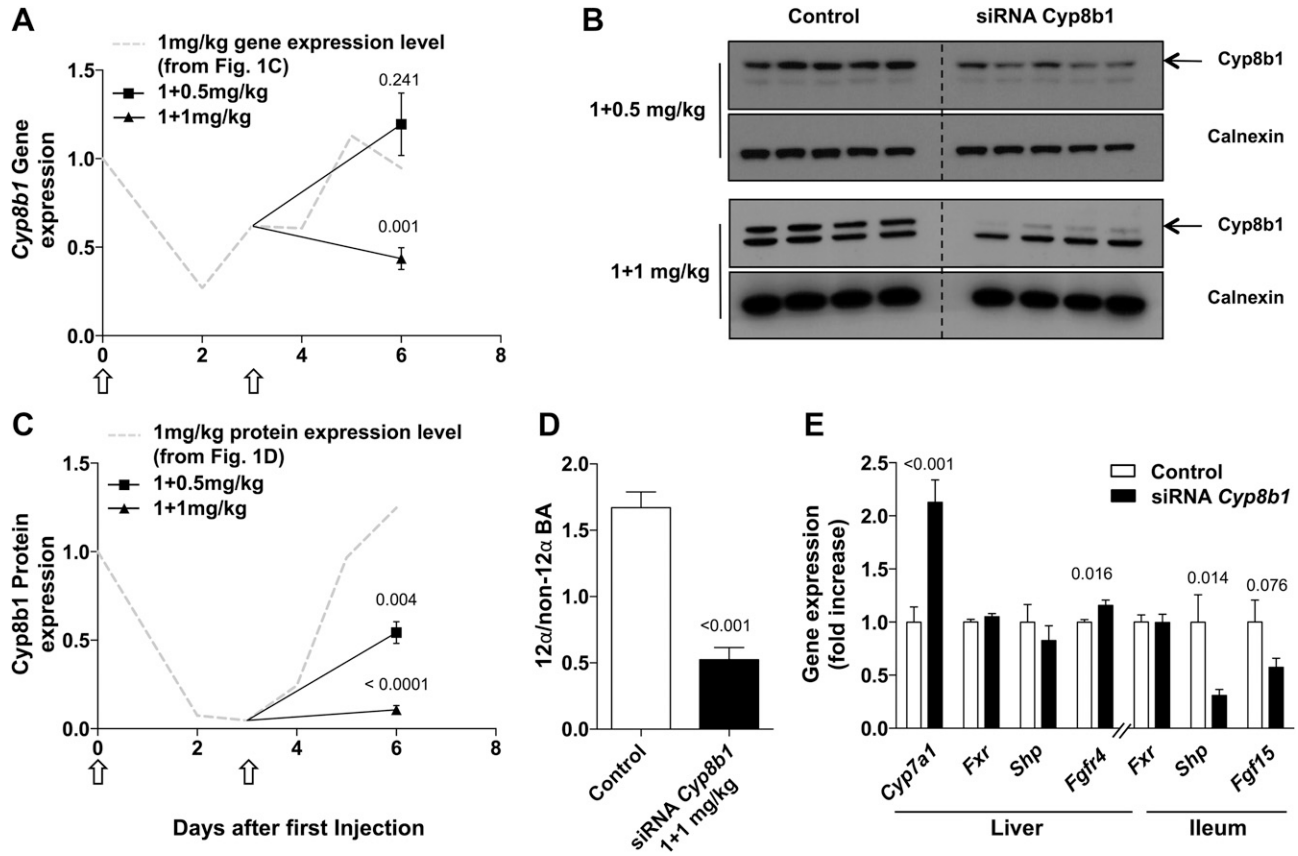

Figure 2. Longer-term *Cyp8b1* KD results in BA pool remodeling. Wild-type (WT) mice received intravenous injections of either PBS or *Cyp8b1* siRNA at d 0 (1 mg/kg) and d 3 (0.5 or 1 mg/kg). *A–C*) Cyp8b1 mRNA (*A*) and protein (*B, C*) expression were assessed at d 6 after the first injection. Cyp8b1 protein was normalized to calnexin. Dashed lines show Cyp8b1 expression levels after a single injection of 1 mg/kg (*A, C*; from Fig. 1*C, D* respectively). White arrows represent siRNA injection time points. Bars represent means ± SEM (n = 4–5 mice). *D*) Plasma BA levels were quantified at d 6 after the first injection and represented as the ratio of 12-α BA in micrometers over non–12-α BA in micromolar. Bars represent means ± SEM from n = 4 mice. *E*) WT mice received intravenous injections of PBS, control, or *Cyp8b1* siRNA (1 mg/kg) every 3 d. Liver and Ileal gene expression levels were assessed between d 6 and 9 after the first injection. Bars represent means ± SEM from n = 9–10 mice from 2 independent experiments. White arrows (*A, C*) indicate intravenous injection time points. Black arrows (*B*) indicate Cyp8b1 protein bands.

pool composition, at the end of the experiment, 3–4 d after mice received the final siRNA injection. Even after 1 mo of siRNA treatment, Cyp8b1 protein levels were still significantly decreased (by 55%) and resulted in significant remodeling of the BA pool (43% reduction in 12α/non–12α-BA ratio; Supplemental Figs. 5 and 6, respectively). We detected no changes in hepatic macrophage content (Supplemental Fig. 7*A*), and mice did not present significant signs of general inflammation as assessed by quantification of circulating neutrophils (Supplemental Fig. 7*B*). Of interest, reduction in hepatic cholesterol was associated with significant inhibition in cholesterol crystal formation (Supplemental Fig. 7*C* and *D*), which has been associated with NASH in humans (39).

As *Cyp8b1* siRNA-injected livers were almost devoid of steatosis, we hypothesized that this effect may not be exclusively attributed to a lack of *de novo* lipid accumulation, but may also be a result of increased removal of preestablished fat from the liver. To confirm our hypothesis, we compared hepatic steatosis before and after treatment with *Cyp8b1* siRNA. We fed mice with HCD for 10 wk, and treated them for an additional 4 wk while on the HCD using our siRNA protocol. After 10 wk of HCD feeding, before beginning siRNA treatment, mice already presented nascent steatosis, which was visible by hematoxylin and eosin staining (**Fig. 5*A, B***). Compared with mice before siRNA treatment, mice that were simultaneously treated with siRNA and HCD for an additional 4 wk presented significantly lower hepatic cholesterol content (Fig. 5*C*), which suggested that *Cyp8b1* KD stimulated the clearance of preexisting cholesterol and was correlated with the increased cholesterol and BA excretion observed in Fig. 3*B, D*. In addition, compared with pre-siRNA treatment, a 35% decrease in hepatic steatosis was observed in the *Cyp8b1* KD group (P = 0.026; Fig. 5*B*); however, in contrast to the significant reduction in hepatic cholesterol, no difference in hepatic triglycerides was observed after *Cyp8b1* siRNA treatment compared with pre-siRNA treatment in the regression experiment (Supplemental Fig. 8). Plasma aspartate transaminase and alanine transaminase levels were within the normal range, similar to levels observed before treatment (Supplemental Fig. 9). Similarly, levels of plasma total and LDL-C were comparable to those observed before treatment (Supplemental Fig. 9). As a control, nontreated mice on HCD for an additional 4 wk continued

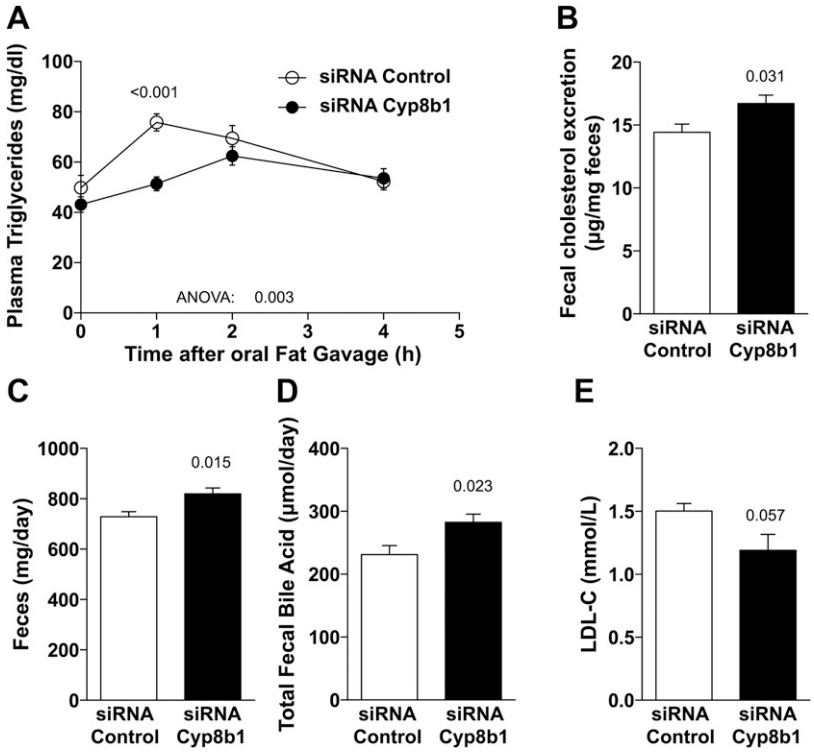

Figure 3. Impact of *Cyp8b1* KD on intestinal fat absorption and fecal lipid and BA excretion. *A*) Wild-type (WT) mice received intravenous injections of either *Cyp8b1* siRNA (black circle) or control siRNA (white circle; 1 mg/kg) at d 0 and 3. Oral Fat gavage was performed at d 6 after the first injection, and fat absorption was assessed by measuring plasma triglyceride levels. Bars represent means ± SEM from n = 6 mice. *B–E*) WT mice fed HCD received injections (1 mg/kg, i.v.) of either *Cyp8b1* siRNA (black bars) or control siRNA (white bars) twice a week. Fecal cholesterol content (*B*), weight of excreted feces (*C*), and fecal BA content (*D*) were assessed 3 wk after the first injection. *E*) Plasma LDL-C was assessed 4 wk after the first injection. Bars represent means ± SEM (n = 6–7 mice).

to accumulate liver cholesterol, liver triglycerides, and steatosis (Fig. 5 and Supplemental Fig. 8), which confirmed the results observed of our previous cohort (Fig. 4) that the silencing of *Cyp8b1* significantly lowers hepatic fat accumulation. Thus, in our study, therapeutic silencing of *Cyp8b1* not only lowered hepatic fat accumulation, but indeed reversed preexisting steatosis.

DISCUSSION

To determine the viability of long-term therapeutic inhibition of *CYP8B1* in adulthood, and to assess whether this inhibition would result in beneficial effects on hepatic fat accumulation and NAFLD, driven by remodeling of the BA pool, we designed an RNAi-based therapeutic protocol to knock down *Cyp8b1* in mice. We successfully achieved the long-term inhibition of hepatic *Cyp8b1 in vivo*, which resulted in remodeling of the BA pool and led to a significant and dramatic decrease in liver steatosis, driven by an increase in fecal excretion of lipids and BAs. Moreover, hepatic cholesterol content and steatosis were significantly lower after treatment compared with pretreatment, which suggests that, in addition to reducing hepatic fat accumulation, *Cyp8b1* inhibition resulted in regression of preexisting hepatic cholesterol. Our data demonstrate that long-term therapeutic inhibition of *Cyp8b1* results in remodeling of the BA pool and may be an effective target to prevent and regress NAFLD.

Compared with the lifetime disruption of *Cyp8b1* in *Cyp8b1*$^{-/-}$ mice, we determined in this study the dynamic effect of BA pool remodeling in adulthood over a short period of time. Our approach allowed us to evaluate the potential of transient modulation of Cyp8b1, which could be of interest for the development of therapeutics and for their translation to the clinic. Beyond a therapeutic proof of concept, our approach also allowed for investigation of the effects of the dynamic reshaping of the BA pool, independent of any compensatory mechanisms that occur in *Cyp8b1*$^{-/-}$ mice. Indeed, a recent study found that *Cyp8b1*$^{+/-}$ mice exhibit mild BA remodeling—significant changes in only HDCA and α-MCA, with no decrease, and in fact, a mild increase in CA—compared with their *Cyp8b1*$^{+/+}$ counterparts, associated with no changes in NAFLD development (32), which suggests that a robust reduction of Cyp8b1 is needed to sufficiently remodel the BA pool to observe a phenotype. Our findings emphasize that a reduction in CA levels by ~51% (Supplemental Fig. 6), as opposed to complete elimination of CA as in *Cyp8b1*$^{-/-}$ mice, is sufficient to decrease liver cholesterol content. By using our approach, we recapitulated the increase in hepatic *Cyp7a1* expression and remodeling of the BA pool observed in adult *Cyp8b1*$^{-/-}$ mice after only 6 d of *Cyp8b1* KD. The increase in *Cyp7a1* expression, together with the increase in fecal BA excretion, suggest that BA synthesis and pool size may be increased in the face of *Cyp8b1* KD. We quantified plasma BAs, which are a small fraction of the BA pool and may not accurately reflect the composition of the total BA pool. Quantification of total BA pool size is required to directly determine whether it is altered upon *Cyp8b1* KD. Of note, BA pool remodeling directly affected fat absorption abilities, as observed in the oral fat tolerance test, also within 6 d of KD. Moreover, as BAs affect intestinal motility (45), the decrease in plasma triglycerides might also be a result of a decrease in intestinal transit time. In addition, our multi-injection protocol was robust enough to maintain these alterations during the 4 wk of *Cyp8b1* inhibition and under chronic

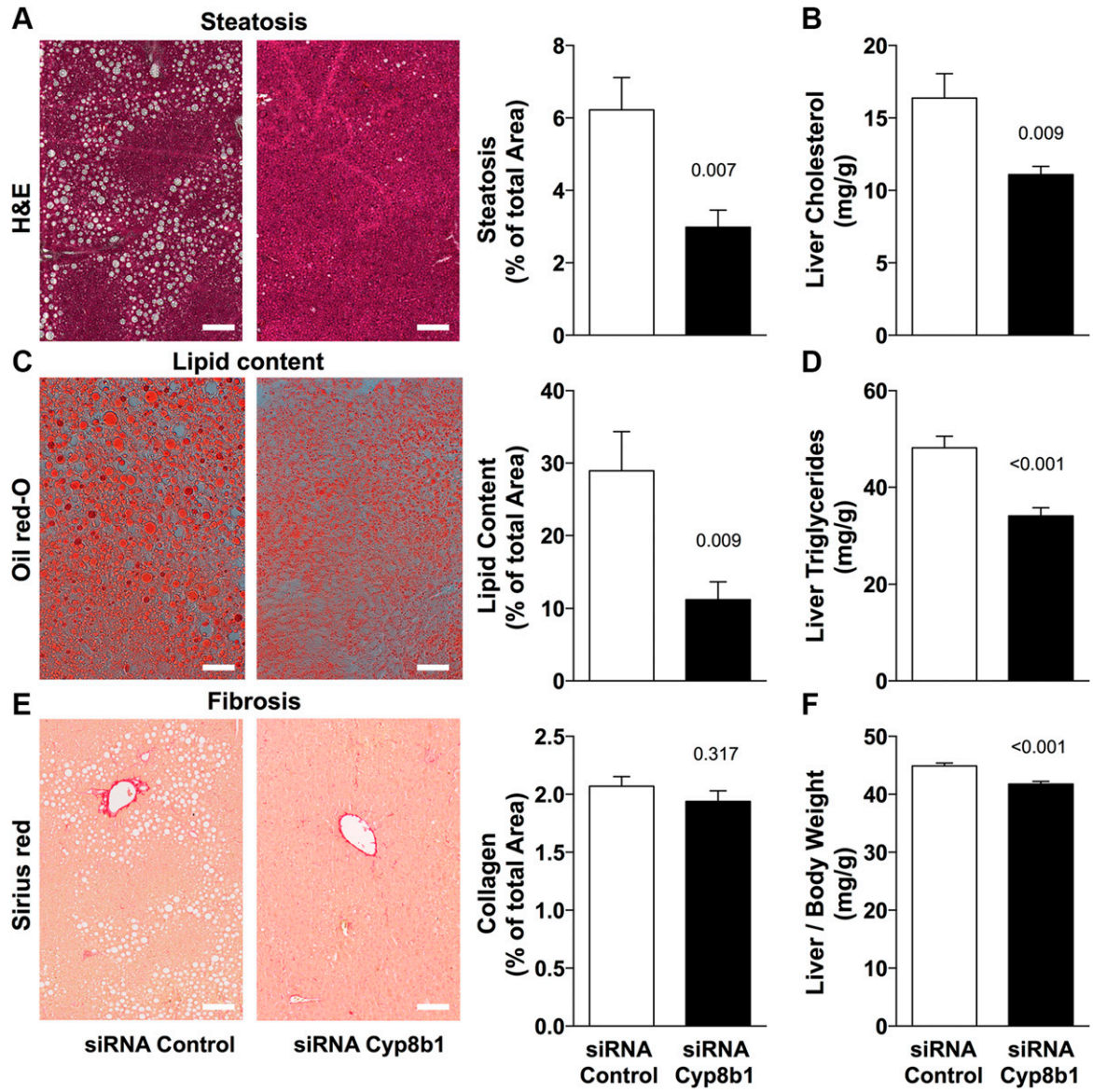

Figure 4. *Cyp8b1* KD lowers hepatic fat accumulation. Wild-type (WT) mice fed HCD for 15 wk received injections (1 mg/kg, i.v.) of either *Cyp8b1* siRNA (black bars) or control siRNA (white bars) twice a week for an additional 4 wk. *A*) Liver steatosis was assessed by hematoxylin and eosin staining. *B–D*) Liver fat accumulation was evaluated by ORO staining (*C*) and by assessing cholesterol (*B*) and triglyceride (*D*) content in liver lipid extracts. *E*) Liver fibrosis was assessed by Sirius red staining for collagen fibers. *F*) Liver weights. Bars represent means ± SEM (n = 6–7 mice). Scale bars, 100 μm (*A*, *E*); 50 μm (*C*).

HCD conditions. Indeed, we observed a 16% increase in cholesterol excretion after 3 wk of *Cyp8b1* KD in mice that were fed HCD compared with the ~50% increase in fecal neutral sterol content that resulted from the lifetime disruption of *Cyp8b1* in *Cyp8b1*$^{-/-}$ mice (27). Despite the modest impact on intestinal fat absorption, *Cyp8b1* inhibition reduced hepatic steatosis by 52%, which indicates that longer treatment protocols would have a higher impact on hepatic lipid accumulation and suggests great potential for the development of synthetic inhibitors that target Cyp8b1.

HCD feeding promotes NAFLD in rabbits (46). In addition, *Cyp8b1*$^{-/-}$ mice demonstrated reduced intestinal fat absorption when fed HCD (29). Thus, we used HCD (0.5% cholesterol) to elicit hepatic fat accumulation in our mouse model. By inhibiting *Cyp8b1* in mice fed HCD, we conceptually aimed at having an impact at the level of dietary cholesterol absorption by modifying the hydrophilic/lipophilic balance of the BA pool (9), and at the level of cholesterol catabolism by increasing Cyp7a1 (27). In the context of NAFLD/NASH, establishing physiologically relevant animal models *in vivo* is challenging. Methionine-/choline-deficient diets promote fibrosis, but fail to recapitulate the complex metabolic environment of NAFLD (47). HCD, high-fat, and high-sucrose diets result in phenotypes that are more representative of the pathophysiology of NASH, but do not promote severe forms of liver fibrosis, at least in relatively short periods of time (47). Additional studies are required to validate the Cyp8b1-mediated reduction in fat accumulation in the liver as a versatile therapeutic strategy that targets different clinical stages of fatty liver disease.

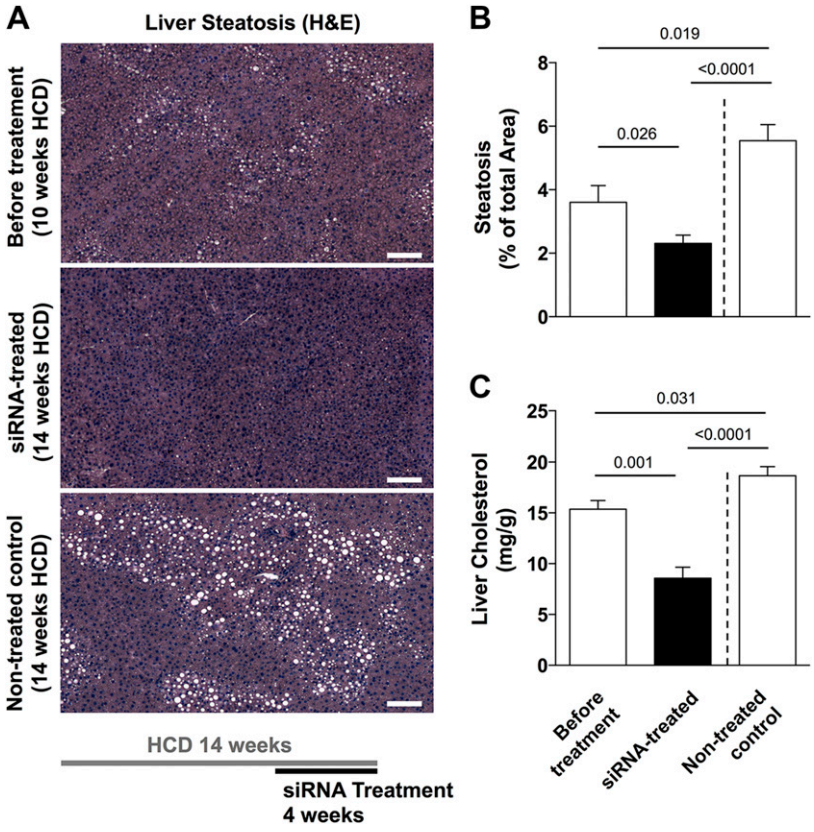

Figure 5. *Cyp8b1* KD results in the regression of NAFLD. Wild-type (WT) mice fed HCD for 10 wk received intravenous injections of either *Cyp8b1* siRNA (1 mg/kg) or PBS twice a week for an additional 4 wk. *A–C*) Steatosis (*A*, *B*) and cholesterol content (*C*) were assessed in livers from mice that were euthanized before the beginning of treatment (10 wk on HCD) or from mice that were treated with either siRNA or PBS (14 wk on HCD). *A*) Representative images of liver steatosis quantified in panel *B*. Scale bars, 100 μm (*A*). Bars represent means ± SEM [n = 10–16 liver slices from 5–8 mice (*B*); n = 5–8 mice (*C*)].

BA metabolism differs between humans and mice; thus, some consideration is needed before the direct translation of our findings to humans. One important difference between humans and mice is that, in humans, CDCA is a major primary BA, whereas in mice, CDCA is metabolized to MCA in the liver. CDCA is the most potent BA agonist for FXR, which suggests that, in humans, as opposed to mice, increased hepatic FXR signaling would be observed. In the intestine in humans, CDCA is modified to lithocholic acid, a less potent FXR agonist (16); however, in mice, tauro-β-MCA acts as an FXR antagonist (48). Thus, it is expected that increased FXR agonism would be observed in both the liver and the intestine of humans compared with mice. In our mouse model, we did not observe any changes in hepatic FXR signaling at the RNA level; however, we observed a decrease in intestinal Fxr activity as evidenced by a significant reduction in the Fxr-regulated genes, *Shp* and *Fgf15* (27, 48), possibly caused by an increase in the Fxr antagonist, tauro-β-MCA. This decrease in intestinal Fxr activity correlates with the increase in Cyp7a1 in the liver. This is in agreement with previous studies that used tissue-specific Fxr knockout mice, which suggests that the intestinal Fxr–Fgf15 axis is more important for Cyp7a1 regulation compared with the liver Fxr–Shp axis (49).

Our study highlights the feasibility of nucleic acid therapy in targeting the BA pool. siRNA treatment for 4 wk led to a dramatic reduction in hepatic cholesterol accumulation and steatosis. The emergence of modified RNAs, siRNAs, or antisense oligonucleotides, along with new classes of delivery vectors, is promising (35). Their increased circulation time and enhanced targeting properties, which are associated with increased stability and decreased toxicity of new generations of nucleic acids, should improve the efficacy of therapies that target high-turnover proteins, such as CYP8B1. Indeed, a recent study that targeted proprotein convertase subtilisin/kexin type 9 in humans by using a single subcutaneous injection of siRNA conjugated to triantennary *N*-acetylgalactosamine carbohydrates to enhance hepatocyte targeting decreased plasma proprotein convertase subtilisin/kexin type 9 and LDL-C for 6 mo without promoting severe adverse effects (36).

Overall, we find here that the therapeutic inhibition of *Cyp8b1* in mice results in remodeling of the BA pool, which alters both its signaling and physicochemical properties, and leads to the reduction and regression of NAFLD, modulated, in part, *via* a reduction in intestinal fat absorption. Thus, inhibition of CYP8B1 may be a valuable therapeutic target for the treatment of NAFLD. FJ

ACKNOWLEDGMENTS

Microscopy images were acquired at the Image Microscopy Unit [Institute of Medical Biology, Agency for Science, Technology, and Research (A*STAR)]. Funding was provided by A*STAR and the National University of Singapore. The authors declare no conflicts of interest.

AUTHOR CONTRIBUTIONS

R. Chevre and L. Trigueros-Motos designed the study, designed, performed, and analyzed experiments, and

wrote the manuscript; D. Castaño contributed to NAFLD study design, performed and analyzed experiments; T. Chua performed NAFLD sample analysis; L. Trigueros-Motos, M. Corlianò, L. Sim, and L. Sng performed and quantified immunohistology experiments; J. V. Patankar contributed to experiment design and reviewed the manuscript; T. L. Juin helped with animal experiments; G. Carissimo and L. F. P. Ng performed and analyzed flow cytometry experiments; C. N. J. Yi and C. C. Eliathamby performed quantitative PCR analysis; A. K. Groen analyzed experiments and reviewed the manuscript; and M. R. Hayden and R. R. Singaraja designed experiments, supervised the study, and reviewed the manuscript.

REFERENCES

1. Adams, L. A., Lymp, J. F., St Sauver, J., Sanderson, S. O., Lindor, K. D., Feldstein, A., and Angulo, P. (2005) The natural history of nonalcoholic fatty liver disease: a population-based cohort study. *Gastroenterology* **129**, 113–121
2. Wierzbicki, A. S., and Oben, J. (2012) Nonalcoholic fatty liver disease and lipids. *Curr. Opin. Lipidol.* **23**, 345–352
3. Lazo, M., and Clark, J. M. (2008) The epidemiology of nonalcoholic fatty liver disease: a global perspective. *Semin. Liver Dis.* **28**, 339–350
4. Zezos, P., and Renner, E. L. (2014) Liver transplantation and non-alcoholic fatty liver disease. *World J. Gastroenterol.* **20**, 15532–15538
5. Lefebvre, P., Cariou, B., Lien, F., Kuipers, F., and Staels, B. (2009) Role of bile acids and bile acid receptors in metabolic regulation. *Physiol. Rev.* **89**, 147–191
6. Staels, B., and Fonseca, V. A. (2009) Bile acids and metabolic regulation: mechanisms and clinical responses to bile acid sequestration. *Diabetes Care* **32** (Suppl 2), S237–S245
7. Hylemon, P. B., Zhou, H., Pandak, W. M., Ren, S., Gil, G., and Dent, P. (2009) Bile acids as regulatory molecules. *J. Lipid Res.* **50**, 1509–1520
8. Hofmann, A. F., and Roda, A. (1984) Physicochemical properties of bile acids and their relationship to biological properties: an overview of the problem. *J. Lipid Res.* **25**, 1477–1489
9. Wang, D. Q., Tazuma, S., Cohen, D. E., and Carey, M. C. (2003) Feeding natural hydrophilic bile acids inhibits intestinal cholesterol absorption: studies in the gallstone-susceptible mouse. *Am. J. Physiol. Gastrointest. Liver Physiol.* **285**, G494–G502
10. Makishima, M., Okamoto, A. Y., Repa, J. J., Tu, H., Learned, R. M., Luk, A., Hull, M. V., Lustig, K. D., Mangelsdorf, D. J., and Shan, B. (1999) Identification of a nuclear receptor for bile acids. *Science* **284**, 1362–1365
11. Parks, D. J., Blanchard, S. G., Bledsoe, R. K., Chandra, G., Consler, T. G., Kliewer, S. A., Stimmel, J. B., Willson, T. M., Zavacki, A. M., Moore, D. D., and Lehmann, J. M. (1999) Bile acids: natural ligands for an orphan nuclear receptor. *Science* **284**, 1365–1368
12. Wang, H., Chen, J., Hollister, K., Sowers, L. C., and Forman, B. M. (1999) Endogenous bile acids are ligands for the nuclear receptor FXR/BAR. *Mol. Cell* **3**, 543–553
13. Kawamata, Y., Fujii, R., Hosoya, M., Harada, M., Yoshida, H., Miwa, M., Fukusumi, S., Habata, Y., Itoh, T., Shintani, Y., Hinuma, S., Fujisawa, Y., and Fujino, M. (2003) A G protein-coupled receptor responsive to bile acids. *J. Biol. Chem.* **278**, 9435–9440
14. Maruyama, T., Miyamoto, Y., Nakamura, T., Tamai, Y., Okada, H., Sugiyama, E., Nakamura, T., Itadani, H., and Tanaka, K. (2002) Identification of membrane-type receptor for bile acids (M-BAR). *Biochem. Biophys. Res. Commun.* **298**, 714–719
15. Thomas, C., Auwerx, J., and Schoonjans, K. (2008) Bile acids and the membrane bile acid receptor TGR5—connecting nutrition and metabolism. *Thyroid* **18**, 167–174
16. Schaap, F. G., Trauner, M., and Jansen, P. L. (2014) Bile acid receptors as targets for drug development. *Nat. Rev. Gastroenterol. Hepatol.* **11**, 55–67
17. Out, C., Groen, A. K., and Brufau, G. (2012) Bile acid sequestrants: more than simple resins. *Curr. Opin. Lipidol.* **23**, 43–55
18. Trauner, M., Claudel, T., Fickert, P., Moustafa, T., and Wagner, M. (2010) Bile acids as regulators of hepatic lipid and glucose metabolism. *Dig. Dis.* **28**, 220–224
19. Thomas, C., Gioiello, A., Noriega, L., Strehle, A., Oury, J., Rizzo, G., Macchiarulo, A., Yamamoto, H., Mataki, C., Pruzanski, M., Pellicciari, R., Auwerx, J., and Schoonjans, K. (2009) TGR5-mediated bile acid sensing controls glucose homeostasis. *Cell Metab.* **10**, 167–177
20. Watanabe, M., Houten, S. M., Mataki, C., Christoffolete, M. A., Kim, B. W., Sato, H., Messaddeq, N., Harney, J. W., Ezaki, O., Kodama, T., Schoonjans, K., Bianco, A. C., and Auwerx, J. (2006) Bile acids induce energy expenditure by promoting intracellular thyroid hormone activation. *Nature* **439**, 484–489
21. Wang, Y. D., Chen, W. D., Yu, D., Forman, B. M., and Huang, W. (2011) The G-protein-coupled bile acid receptor, Gpbar1 (TGR5), negatively regulates hepatic inflammatory response through antagonizing nuclear factor κ light-chain enhancer of activated B cells (NF-κB) in mice. *Hepatology* **54**, 1421–1432
22. Yuan, L., and Bambha, K. (2015) Bile acid receptors and nonalcoholic fatty liver disease. *World J. Hepatol.* **7**, 2811–2818
23. Porez, G., Prawitt, J., Gross, B., and Staels, B. (2012) Bile acid receptors as targets for the treatment of dyslipidemia and cardiovascular disease. *J. Lipid Res.* **53**, 1723–1737
24. Thomas, C., Pellicciari, R., Pruzanski, M., Auwerx, J., and Schoonjans, K. (2008) Targeting bile-acid signalling for metabolic diseases. *Nat. Rev. Drug Discov.* **7**, 678–693
25. Haeusler, R. A., Astiarraga, B., Camastra, S., Accili, D., and Ferrannini, E. (2013) Human insulin resistance is associated with increased plasma levels of 12α-hydroxylated bile acids. *Diabetes* **62**, 4184–4191
26. Haeusler, R. A., Pratt-Hyatt, M., Welch, C. L., Klaassen, C. D., and Accili, D. (2012) Impaired generation of 12-hydroxylated bile acids links hepatic insulin signaling with dyslipidemia. *Cell Metab.* **15**, 65–74
27. Li-Hawkins, J., Gåfvels, M., Olin, M., Lund, E. G., Andersson, U., Schuster, G., Björkhem, I., Russell, D. W., and Eggertsen, G. (2002) Cholic acid mediates negative feedback regulation of bile acid synthesis in mice. *J. Clin. Invest.* **110**, 1191–1200
28. Slätis, K., Gåfvels, M., Kannisto, K., Ovchinnikova, O., Paulsson-Berne, G., Parini, P., Jiang, Z. Y., and Eggertsen, G. (2010) Abolished synthesis of cholic acid reduces atherosclerotic development in apolipoprotein E knockout mice. *J. Lipid Res.* **51**, 3289–3298
29. Kaur, A., Patankar, J. V., de Haan, W., Ruddle, P., Wijesekara, N., Groen, A. K., Verchere, C. B., Singaraja, R. R., and Hayden, M. R. (2015) Loss of Cyp8b1 improves glucose homeostasis by increasing GLP-1. *Diabetes* **64**, 1168–1179
30. Li, P., Ruan, X., Yang, L., Kiesewetter, K., Zhao, Y., Luo, H., Chen, Y., Gucek, M., Zhu, J., and Cao, H. (2015) A liver-enriched long non-coding RNA, lncLSTR, regulates systemic lipid metabolism in mice. *Cell Metab.* **21**, 455–467
31. Bonde, Y., Eggertsen, G., and Rudling, M. (2016) Mice abundant in muricholic bile acids show resistance to dietary induced steatosis, weight gain, and to impaired glucose metabolism. *PLoS One* **11**, e0147772
32. Bertaggia, E., Jensen, K. K., Castro-Perez, J., Xu, Y., Di Paolo, G., Chan, R. B., Wang, L., and Haeusler, R. A. (2017) Cyp8b1 ablation prevents Western diet-induced weight gain and hepatic steatosis because of impaired fat absorption. *Am. J. Physiol. Endocrinol. Metab.* **313**, E121–E133
33. Puri, P., Daita, K., Joyce, A., Mirshahi, F., Santhekadur, P. K., Cazanave, S., Luketic, V. A., Siddiqui, M. S., Boyett, S., Min, H. K., Kumar, D. P., Kohli, R., Zhou, H., Hylemon, P. B., Contos, M. J., Idowu, M., and Sanyal, A. J. (2017) The presence and severity of nonalcoholic steatohepatitis is associated with specific changes in circulating bile acids. *Hepatology* **67**, 534–548
34. Fitzgerald, K., Frank-Kamenetsky, M., Shulga-Morskaya, S., Liebow, A., Bettencourt, B. R., Sutherland, J. E., Hutabarat, R. M., Clausen, V. A., Karsten, V., Cehelsky, J., Nochur, S. V., Kotelianski, V., Horton, J., Mant, T., Chiesa, J., Ritter, J., Munisamy, M., Vaishnaw, A. K., Gollob, J. A., and Simon, A. (2014) Effect of an RNA interference drug on the synthesis of proprotein convertase subtilisin/kexin type 9 (PCSK9) and the concentration of serum LDL cholesterol in healthy volunteers: a randomised, single-blind, placebo-controlled, phase 1 trial. *Lancet* **383**, 60–68
35. Wittrup, A., and Lieberman, J. (2015) Knocking down disease: a progress report on siRNA therapeutics. *Nat. Rev. Genet.* **16**, 543–552
36. Fitzgerald, K., White, S., Borodovsky, A., Bettencourt, B. R., Strahs, A., Clausen, V., Wijngaard, P., Horton, J. D., Taubel, J., Brooks, A., Fernando, C., Kauffman, R. S., Kallend, D., Vaishnaw, A., and Simon,

A. (2017) A highly durable RNAi therapeutic inhibitor of PCSK9. *N. Engl. J. Med.* **376**, 41–51
37. Barteau, B., Chèvre, R., Letrou-Bonneval, E., Labas, R., Lambert, O., and Pitard, B. (2008) Physicochemical parameters of non-viral vectors that govern transfection efficiency. *Curr. Gene Ther.* **8**, 313–323
38. Schmittgen, T. D., and Livak, K. J. (2008) Analyzing real-time PCR data by the comparative C_T method. *Nat. Protoc.* **3**, 1101–1108
39. Ioannou, G. N., Haigh, W. G., Thorning, D., and Savard, C. (2013) Hepatic cholesterol crystals and crown-like structures distinguish NASH from simple steatosis. *J. Lipid Res.* **54**, 1326–1334
40. Pathak, P., Li, T., and Chiang, J. Y. (2013) Retinoic acid-related orphan receptor α regulates diurnal rhythm and fasting induction of sterol 12α-hydroxylase in bile acid synthesis. *J. Biol. Chem.* **288**, 37154–37165
41. Yamada, M., Nagatomo, J., Setoguchi, Y., Kuroki, N., Higashi, S., and Setoguchi, T. (2000) Circadian rhythms of sterol 12alpha-hydroxylase, cholesterol 7alpha-hydroxylase and DBP involved in rat cholesterol catabolism. *Biol. Chem.* **381**, 1149–1153
42. Eguchi, A., De Mollerat Du Jeu, X., Johnson, C. D., Nektaria, A., and Feldstein, A. E. (2016) Liver Bid suppression for treatment of fibrosis associated with non-alcoholic steatohepatitis. *J. Hepatol.* **64**, 699–707
43. Goodwin, B., Jones, S. A., Price, R. R., Watson, M. A., McKee, D. D., Moore, L. B., Galardi, C., Wilson, J. G., Lewis, M. C., Roth, M. E., Maloney, P. R., Willson, T. M., and Kliewer, S. A. (2000) A regulatory cascade of the nuclear receptors FXR, SHP-1, and LRH-1 represses bile acid biosynthesis. *Mol. Cell* **6**, 517–526
44. Inagaki, T., Choi, M., Moschetta, A., Peng, L., Cummins, C. L., McDonald, J. G., Luo, G., Jones, S. A., Goodwin, B., Richardson, J. A., Gerard, R. D., Repa, J. J., Mangelsdorf, D. J., and Kliewer, S. A. (2005) Fibroblast growth factor 15 functions as an enterohepatic signal to regulate bile acid homeostasis. *Cell Metab.* **2**, 217–225
45. Bajor, A., Gillberg, P. G., and Abrahamsson, H. (2010) Bile acids: short and long-term effects in the intestine. *Scand. J. Gastroenterol.* **45**, 645–664
46. Kim, E. J., Kim, B. H., Seo, H. S., Lee, Y. J., Kim, H. H., Son, H. H., and Choi, M. H. (2014) Cholesterol-induced non-alcoholic fatty liver disease and atherosclerosis aggravated by systemic inflammation. *PLoS One* **9**, e97841
47. Machado, M. V., Michelotti, G. A., Xie, G., Almeida Pereira, T., Boursier, J., Bohnic, B., Guy, C. D., and Diehl, A. M. (2015) Mouse models of diet-induced nonalcoholic steatohepatitis reproduce the heterogeneity of the human disease. *PLoS One* **10**, e0127991
48. Sayin, S. I., Wahlström, A., Felin, J., Jäntti, S., Marschall, H. U., Bamberg, K., Angelin, B., Hyötyläinen, T., Orešič, M., and Bäckhed, F. (2013) Gut microbiota regulates bile acid metabolism by reducing the levels of tauro-beta-muricholic acid, a naturally occurring FXR antagonist. *Cell Metab.* **17**, 225–235
49. Kim, I., Ahn, S. H., Inagaki, T., Choi, M., Ito, S., Guo, G. L., Kliewer, S. A., and Gonzalez, F. J. (2007) Differential regulation of bile acid homeostasis by the farnesoid X receptor in liver and intestine. *J. Lipid Res.* **48**, 2664–2672

Received for publication October 3, 2017.
Accepted for publication February 5, 2018.